*Proceedings of the 21st ICSMGE, Vienna, Austria, 14 – 19 June 2026. Pistrol, Adam & Schweiger (eds.)*
*Published by: ÖGG, Austrian Society for Geomechanics, Salzburg, Austria, ISBN 978-3-9503898-4-5*
*https://doi.org/10.53243/ICSMGE2026-2232*

# Cyclic behavior of geotextile-encased sand: resistance, stiffness and energy dissipation

Hyeong-Joo Kim
*Dept. of Civil Eng., Kunsan Nat'l Univ., Saemangeum Campus, Head Professor, South Korea*

Seokjae Lee
*Dept. of Civil Eng., Kunsan Nat'l Univ., Assistant Professor, South Korea*

Hyeong-Soo Kim, Tae-Wong Park
*Renewable Energy Research Inst., Kunsan Nat'l Univ., South Korea*

Tae-Eon Kim, Choi Soo-Woong, **Voltaire Anthony Jr Corsino**, James Vincent Reyes
*Dept. of Civil & Environ. Eng., Kunsan Nat'l Univ., South Korea, vacorsino@kunsan.ac.kr*

ABSTRACT: This study investigates the cyclic and post-cyclic behavior of sand specimens encased in geotextile fabric, focusing on resistance, stiffness retention, and energy dissipation. 15 cyclic triaxial tests were conducted on silty sand at relative densities of 35% and 50%, under an effective confining pressure of 100 kPa. Specimens were tested in unencased and encased configurations at cyclic stress ratios (*CSR*) of 0.15–0.30. Additionally, three special loading cases where conducted: (a) undrained cyclic loading followed by immediate monotonic loading, (b) cyclic loading with reconsolidation before monotonic loading, and (c) drained monotonic preload followed by cyclic loading. Encasement significantly reduced axial strain accumulation and delayed stiffness degradation, with the greatest benefit at lower *CSR* values. At *CSR* = 0.15, encased specimens (*DR* = 35%) endured nearly ten times more cycles to the softening threshold compared to unencased specimens. Cyclic resistance curves and normalized dissipated energy ($DE_N$) values indicated that encasement increased the number of cycles to liquefaction, slowed energy dissipation growth, and delayed pore pressure build-up. Post-liquefaction tests showed that reconsolidation improved strength through densification but repeated cyclic events caused residual stiffness loss due to degradation of soil–fabric interaction. These results demonstrate the effectiveness of geotextile encasement in enhancing cyclic performance and post-liquefaction recovery in silty sands.

KEYWORDS: Geosynthetic, cyclic loading, post-cyclic loading, soil softening.

## 1 INTRODUCTION

Geotextile encasement is a widely applied method to improve the mechanical performance of soils under static and cyclic loading. By mobilizing tensile resistance in the fabric, geotextiles confine the soil mass, suppress lateral deformations, and enhance bearing capacity (Raithel et al. 2002; Kim et al. 2024). Applications include geosynthetic-encased stone columns (GESCs), geotextile tubes for embankment foundations, and soilbags used in coastal and seismic environments (Lawson 2008; Kim et al. 2023; Matsuoka et al. 2004). While numerous studies demonstrate the benefits of encasement in clean sands and gravels, the coupled behavior between cyclic softening of soil and tensile confinement by the fabric remains insufficiently quantified. In particular, under undrained cyclic conditions, pore pressure buildup critically reduces effective stress (Seed et al. 1985; Boulanger and Ziotopoulou 2015), and it is unclear how confinement influences soil stiffness degradation and energy dissipation when drainage is limited. To address this gap, this study investigates geotextile-encased sand under different cyclic–static loading histories using a cyclic triaxial apparatus. The experimental program comprises 15 tests, including baseline cyclic tests on both encased and unencased sand at multiple relative densities and cyclic stress ratio (*CSR*) levels, and three special loading sequences designed to simulate realistic field scenarios. These loading paths, illustrated in Figure 1, include:

(1) *Immediate undrained monotonic loading after cyclic load (SC-1)*. This case represents situations where a permanent or static load is applied directly after a cyclic disturbance, while pore pressures remain elevated and soil strength is temporarily reduced. Examples include seismic shaking of soilbag walls followed by backfill placement, or rapid cyclic wave action on coastal geotextile tubes followed by a high water level or overtopping. In foundation applications, an encased sand column vibrated by traffic may suddenly receive a heavy axle load. In all cases, the soil must resist a static surcharge in a weakened undrained state, making this one of the most critical loading histories.

(2) *Drained reconsolidated monotonic loading after cyclic loads (SC-2).* This case reflects situations where the encased soil undergoes cyclic disturbance but is given time to reconsolidate before subsequent loading. In coastal geotextile tubes, cyclic wave action may be followed by a calm period, allowing pore pressures to dissipate before the structure receives a permanent surcharge, such as armor stone placement. In soilbag retaining structures, seismic shaking may temporarily weaken the foundation, but reconsolidation restores effective stress before long-term static loading. In encased sand columns beneath embankments, traffic-induced cyclic strains can occur in early construction stages, followed by reconsolidation under sustained preload.

From a practical standpoint, reconsolidation improves stability by restoring effective stress, but it also causes internal rearrangement of the soil matrix, as dense sands tend to loosen while loose sands densify. This process can lead to subtle changes in the encasement, such as wrinkling or slackening, which may influence how confinement is re-mobilized in the next loading stage. Designers must therefore consider both the benefits of regained strength and the possible alterations in soil–fabric interaction over the service life.

(3) *Heavily preloaded configurations subjected to cyclic load (SC-3).* This case represents encased systems that have undergone substantial preload under drained conditions, such

as the base of soilbag walls, geotextile tubes supporting armor stone, or encased sand columns beneath embankments. Preloading consolidates and densifies the soil matrix while mobilizing tensile forces in the encasement, creating a stable "hardened" initial state.

In this condition, subsequent cyclic loading generates only minimal strains and limited pore pressure rise, as deformation is resisted by both the densified soil skeleton and the pre-tensioned fabric. The cyclic response is therefore characterized by improved resistance, slower stiffness degradation, and reduced tendency toward softening compared to lightly preloaded systems.

For design, this scenario demonstrates the most stable configuration for geotextile-encased soil under cyclic conditions. However, even with heavy preload, long-term degradation remains possible under severe seismic or repetitive loading, and cyclic durability must still be evaluated.

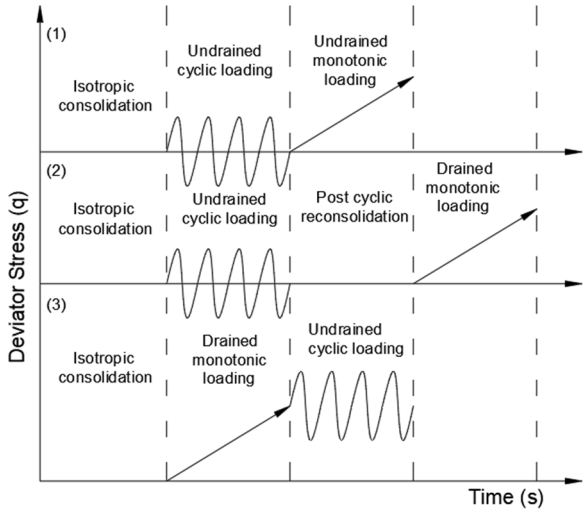


Figure 1. Loading sequence

## 2 TESTING PROGRAM

### 2.1 *Materials*

Soil material used in this set-up was obtained from the geotextile tube test bed in Saemangeum, South Korea with a USCS classification of SM with internal friction angle of 32˚ at relative density, *DR*, of 35% and a non-cohesive fines content of 14%. Encasing fabric consists of a polyethylene geotextile fabric with an ultimate seam strength of 64 kN/m at 9.67% strain. A low strain stiffness of 350 kN/m/m at 5% tensile strain obtained from results is deemed appropriate by the authors for the cyclic loading considerations while for static considerations it is 660kN/m/m. Specimen is prepared via the moist tamping method with the encasing fabric lined inside the wall of the vacuum mold.

### 2.2 *Test Program*

All test specimens for unencased and *J* for encased. Values are in Table 1.

Table 1. Test Specimens

| Designation | Dr(%) | CSR |
|---|---|---|
| DRCSR | 35 | 0.15, 0.20, 0.25 |
| DRCSR | 50 | 0.20, 0.25, 0.30 |
| SC-1, 2, 3 | 35 | 0.20 |

## 3 RESULTS AND DISCUSSION

### 3.1 *Deformation and degradation resistance*

As a load is applied in the major principal direction, it is transferred to the minor principal axis through the soil matrix and then to the encasing fabric via mobilized tensile forces. The fabric confines the soil matrix against itself, restricting lateral deformation. This mechanism also operates under cyclic loading; however, during undrained cyclic conditions, particle rearrangement can cause the fabric to lose some effectiveness due to sliding or micro-wrinkling. The extent of this effect depends on the applied load, as shown in Figure 2. Higher cyclic loads similarly reduce the number of cycles to softening or liquefaction (when pore pressure ratio *R*u reaches 1.0) for both encased and unencased specimens. Figure 2 presents the axial strain development for $DR_{35}$ specimens under *CSR* = 0.15, 0.20, and 0.25. Across all loading levels, encased specimens (*J*) consistently maintained lower strain amplitudes compared to unencased sand (*SM*). The improvement was most pronounced at *CSR* = 0.15, where the encased specimen accumulated almost negligible strain over 45 cycles, corresponding to a *DA* of only 0.02% compared to 1.84% for the unencased specimen. At *CSR* = 0.20 and *CSR* = 0.25, confinement still reduced deformation, with *DA* reductions from 3.56% to 0.54% and from 4.48% to 1.45%, respectively. For comparison, the encased data in Figure 2 are truncated at the cycle count where the unencased specimen reached the failure criterion to highlight this difference. The damping characteristics follow the same trend as modulus degradation, with confinement effects being most significant at lower cyclic stress ratios.

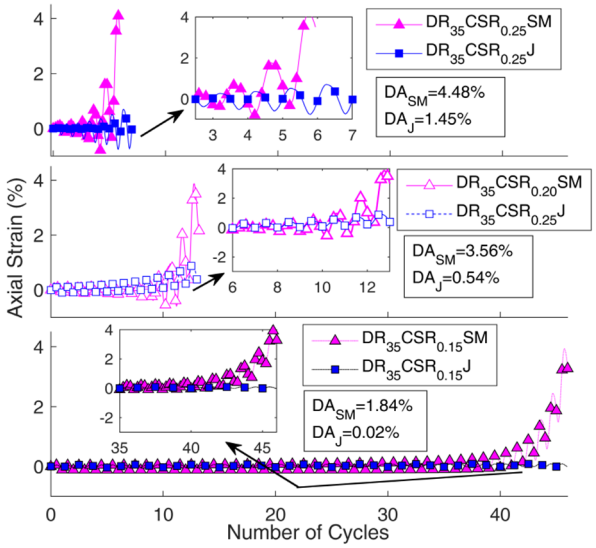


Figure 2. Axial deformation vs cycles

The modulus and damping trends in Figure 3 further emphasize this load-dependent confinement effect. Normalized shear modulus $G/G_{max}$ degradation occurred more slowly in encased specimens, especially at lower CSR values, indicating better retention of stiffness over the loading history. Similarly, normalized damping ratio $D/D_0$ increased at a slower rate for encased specimens, suggesting reduced plastic strain accumulation. However, at higher CSR levels, the advantage of encasement diminished as the soil experienced greater particle rearrangement, reducing the effectiveness of confinement.

These results indicate that geotextile encasement is particularly effective in minimizing cyclic strain accumulation and stiffness loss under low-to-moderate cyclic loads, while benefits reduce under higher load intensities due to accelerated fabric–soil interaction degradation.

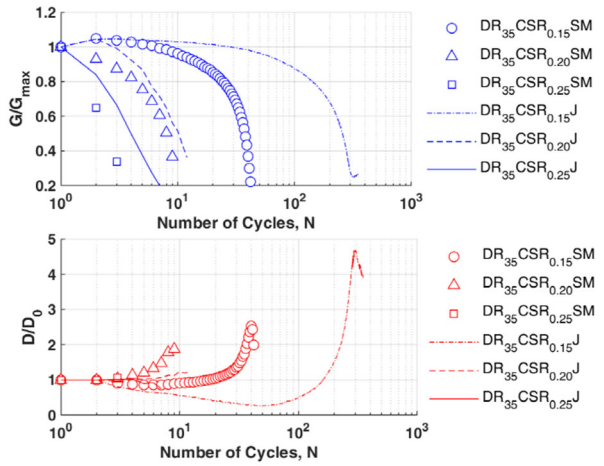


Figure 3. Shear modulus degradation and damping vs cycles

### 3.2 *Pore pressure and energy dissipation*

The cyclic resistance trends in Figure 4 show that encased specimens consistently achieved a higher number of cycles to liquefaction $N_{liq}$ than unencased specimens at equivalent cyclic resistance ratios (*CRR*). At $DR_{35}$, encased specimens sustained up to an order of magnitude more cycles at low CRR values compared to unencased sand, with the gap narrowing as CRR increased. Specifically, at *CRR* = 0.15, encased specimens endured approximately 4.3 times more cycles to liquefaction than unencased specimens, while at *CRR* = 0.25 the improvement was reduced to about 1.7 times. At $DR_{50}$, both materials exhibited improved resistance, though encasement maintained a consistent advantage. The commonly cited benchmark of 200 cycles was exceeded only by encased specimens at the lowest *CRR* levels. Interestingly, the $DR_{35}J$ specimens displayed a resistance curve close to that of ordinary sand at 50% relative density, suggesting that encasement can, in some cases, compensate for lower initial density.

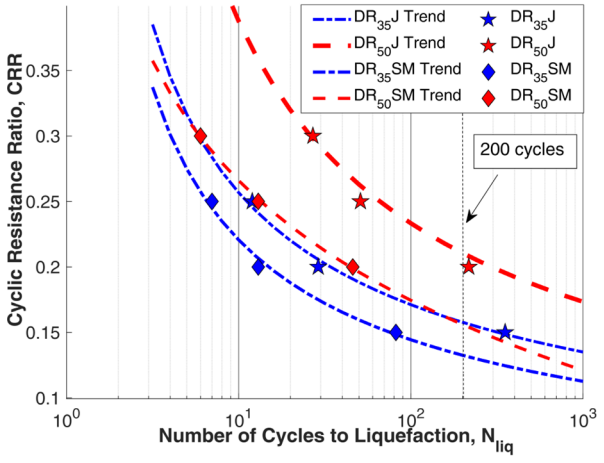


Figure 4. CRR curve

Figure 5 presents the evolution of dissipated energy ($DE_N$) with cycle count, where $DE_N$ represents the accumulated dissipated energy at a given cycle, normalized by the initial effective stress as given in Eq. 1 (following the approach of Green, 2001). In this study, $DE_N$ is distinct from the normalized energy demand (*NED*), which is defined as the total normalized dissipated energy required to reach liquefaction. While Green (2001) normalized *NED* by dividing it by the initial effective stress, here the same normalization is applied to the *DE*, allowing direct comparison of cyclic strain energy accumulation rates.

$$\mathrm{DE_N} = \frac{\frac{1}{2}\sum_{i=1}^{n-1}(\sigma_{d,i+1}+\sigma_{d,i})(\varepsilon_{a,i+1}-\varepsilon_{a,i})}{\sigma_0'} \qquad (1)$$

These findings suggest that confinement not only delays stiffness degradation but also moderates the rate of energy dissipation and associated pore pressure build-up, particularly at lower cyclic stress levels.

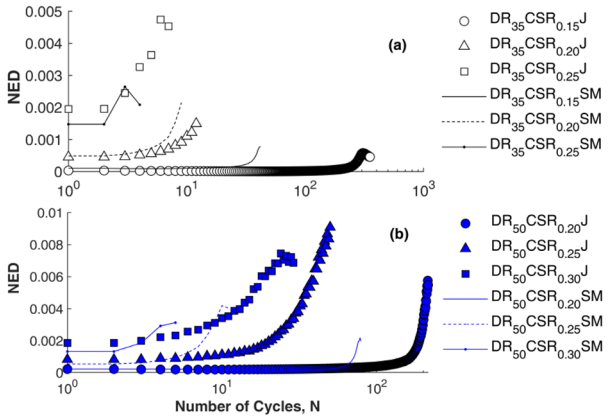


Figure 5. Energy dissipation vs cycles

### 3.3 *Post liquefaction behavior*

Figure 6 compares monotonic stress–strain curves for SC-1 and SC-2 under post-cyclic conditions. Reconsolidation after cyclic loading increased relative density from the initial 35% to between 45.53% and 55.95%, resulting in higher peak strengths compared to the initial condition. However, specimens subjected to multiple cyclic events (SC-1 and SC-2) still exhibited reduced stiffness compared to the purely reconsolidated sample, suggesting partial fabric loosening or residual slackening despite densification.

SC-1, tested under undrained monotonic loading, displayed a relatively softer response at small strains (0–4%), reflecting the near-failure condition of the soil matrix and greater reliance on fabric confinement. In contrast, SC-2 was allowed to reconsolidate before monotonic loading. However, its limited maximum cyclic deformation *DA* of 2.5% (obtained from results) compared to *DA* = 3.56% for the unencased specimen in Figure 2—meant that reconsolidation increased its relative density only to 45.53%, rather than approaching the 55.95% value achieved by the unencased specimen. This smaller density gain partly explains the lower stiffness observed at 4% axial strain. According to the approach of Ishihara and Yoshimine (1992), reconsolidation strains are primarily controlled by the maximum cyclic strain experienced prior to reconsolidation, consistent with these observations. A simple computation using Eq. 2:

$$\sigma_v = K * 2 * v * \varepsilon_1 * J_{gt}/\,Dia \qquad (2)$$

shows a trend closely matching the SC-1 response, further supporting the interpretation that the soil matrix is effectively loose and that the majority of load transfer is carried by the fabric. Here $J_{gt}$ is the geotextile stiffness of 660kN/m/m, Poisson's ratio $v$=0.5 is assumed for undrained conditions, and the coefficient of lateral stress $K$ is taken as 1, implying that nearly all applied load is transferred horizontally to the fabric.

Figure 7 presents the post-liquefaction response for the SC-3 specimen, which was heavily preloaded prior to cyclic loading. This preloading stage densified the soil matrix and mobilized tensile forces in the encasement, creating a

"hardened" initial state. As a result, SC-3 withstood 100 cycles of undrained cyclic loading without reaching liquefaction, in stark contrast to the $DR_{35}CSR_{0}.20J$ specimen in Figure 4, which reached liquefaction after only 29 cycles.

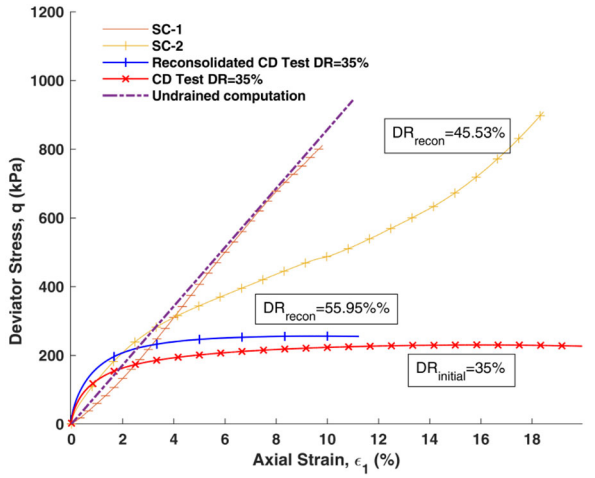


Figure 6. Post shearing reactions

Although undrained loading in SC-3 still produced excess pore pressure build-up, the rate of accumulation was noticeably slower than in the less-dense $DR_{35}CSR_{0}.20J$ case. Effective mean stress decreased gradually rather than collapsing rapidly, and the deviator stress plateaued at a relatively high level, reflecting the combined resistance of the densified soil skeleton and the pre-tensioned geotextile. This behavior underscores the stabilizing effect of preload in delaying pore pressure rise and maintaining cyclic stiffness.

The SC-3 results show that, when encasement is combined with substantial preloading, the system can endure significantly more cyclic loading before softening. However, the persistent, albeit slower, pore pressure build-up suggests that even heavily preloaded encased systems remain vulnerable to degradation under prolonged undrained cyclic conditions.

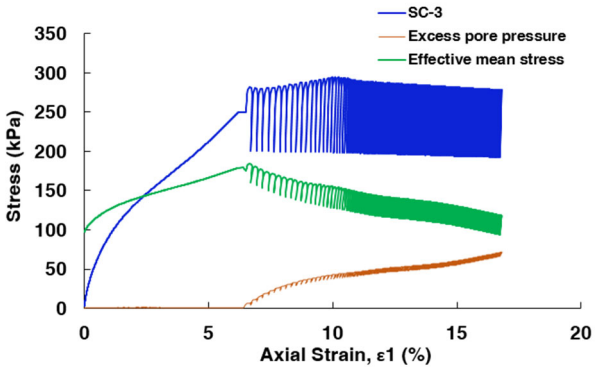


Figure 7. Preloaded encased post shearing reaction

## 4 CONCLUSIONS

Cyclic triaxial tests on geotextile-encased silty sand showed that encasement enhances resistance, stiffness retention, and post-liquefaction recovery across a range of densities and loading histories.

- *Enhanced cyclic performance*. Geotextile encasement reduces cyclic strain accumulation and delays stiffness degradation, particularly at low-to-moderate cyclic stress ratios. This demonstrates the potential of fabric confinement as a mitigation measure against cyclic softening and liquefaction in loose to medium-dense sands.
- *Improved energy efficiency*. Lower normalized energy dissipation rates and delayed pore pressure build-up in encased specimens indicate that confinement promotes elastic energy retention. This behavior can be exploited in design to extend service life and reduce maintenance needs for cyclically loaded geotechnical structures.
- *Post liquefaction resilience.* Even after severe cyclic softening, encasement maintains residual load-carrying capacity. By limiting reconsolidation strains, fabric confinement preserves structural stability under immediate post-liquefaction loads. When reconsolidation is allowed, the soil matrix regains shear strength, reducing reliance on the fabric and delaying full tensile mobilization.

These results quantify the combined effects of soil–fabric interaction, density, and loading history, supporting the use of geosynthetic encasement in seismic or repetitive loading environments. The findings contribute to design knowledge for systems such as stone columns, geotextile tubes, and soilbags, while underscoring the need to assess long-term fabric–soil performance under field-scale cyclic conditions.

## 5 ACKNOWLEDGEMENTS

This research was supported by the Basic Science Research Program through the National Research Foundation of Korea (NRF) funded by the Ministry of Education (RS-2021-NR060134). Additionally, this work was supported by the Human Resources Development of the Korea Institute of Energy Technology Evaluation and Planning(KETEP) grant funded by the Korea government Ministry of Trade, Industry & Energy (No. RS-2021-KP002506).

## 6 REFERENCES

Boulanger, R.W. and Ziotopoulou, K., 2015. PM4Sand (Version 3): A sand plasticity model for earthquake engineering applications. *Center for Geotechnical Modeling Report No. UCD/CGM-15/01, Department of Civil and Environmental Engineering, University of California, Davis, Calif.*

Green, R.A. and Mitchell, J.K., 2004. Energy-based evaluation and remediation of liquefiable soils. In *Geotechnical engineering for transportation projects* (pp. 1961-1970).

Ishihara, K. and Yoshimine, M., 1992. Evaluation of settlements in sand deposits following liquefaction during earthquakes. *Soils and foundations*, *32*(1), pp.173-188.

Kim, H.J., Dinoy, P.R., Reyes, J.V., Kim, H.S., Park, T.W. and Choi, H.S., 2023. Seismic Characteristics of a Geotextile Tube-Reinforced Embankment and Shallow Foundations Laid on Liquefiable Soil. *Applied Sciences*, *13*(2), p.785.

Kim, H.J., Dinoy, P.R., Kim, H.J., Corsino Jr, V.A., Joung, Y.S. and Park, J.Y., 2024. A nonlinear analytical model for consolidated geotextile-encased sand columns. *Geosynthetics International*, *31*(6), pp.981-998.

Lawson, C.R., 2008. Geotextile containment for hydraulic and environmental engineering. *Geosynthetics International*, *15*(6), pp.384-427.

Matsuoka, H., Liu, S., Hasebe, T. and Shimao, R., 2004. Deformation and strength characteristics of soilbag assemblies and their design method. *Journal of the Japan Society of Civil Engineers*, (764), pp.169–181. (in Japanese).

Raithel, M., Kempfert, H.G. and Kirchner, A., 2002, September. Geotextile-encased columns (GEC) for foundation of a dike on very soft soils. In *Proc., 7th Int. Conf. on Geosynthetics* (Vol. 3, pp. 1025-1028). Nice, France: Swets & Zeitlinger.

Seed, H.B., Martin, P.P. and Lysmer, J., 1975. *The generation and dissipation of pore water pressures during soil liquefaction*. College of Engineering, University of California.